

# Time-Varying Entry Heating Profile Replication with a Rotating Arc Jet Test Article

Jay H. Grinstead<sup>1</sup> and Ethiraj Venkatapathy<sup>2</sup>  
*NASA Ames Research Center, Moffett Field, CA 94035*

Eric A. Noyes<sup>3</sup>, Jeffrey J. Mach<sup>4</sup>, and Daniel M. Empey<sup>5</sup>  
*Jacobs Technology Incorporated, NASA Ames Research Center, Moffett Field, CA 94035*

*and*

Dinesh K. Prabhu<sup>6</sup> and Todd R. White<sup>7</sup>  
*ERC Incorporated, Moffett Field, CA 94035*

**A new approach to arc jet testing that replicates the time-varying conditions of atmospheric entry heating was demonstrated. The concept relies on the spatial variation of heat flux and pressure around a cylindrical test article. The spatial variation is transformed to a temporal variation at one location by rotating the test article during exposure to the arc jet stream. The test article rotation mechanism is based on a programmable stepper motor. An entry heat flux profile was mapped to the cylinder's heat flux distribution to determine the rotation angle vs. time executed by the mechanism. A series of arc jet tests with instrumented cylindrical TPS test articles was conducted to prove the concept.**

## I. Introduction

ARC jets are high-enthalpy aeroheating test facilities primarily used to validate the most critical performance parameters of a spacecraft heat shield's thermal protection system (TPS) at conditions simulating atmospheric entry. Arc jet testing of thermal protection materials is typically conducted by exposing a small sample to the arc jet stream for a given duration. Materials scientists and test engineers design a testing configuration to apply a prescribed constant heat flux and surface pressure to an instrumented test model. The data from several tests at a variety of (constant) facility operating conditions are used to develop and validate material response simulations employed for the design of a vehicle's thermal protection system. In flight, however, a spacecraft's heat shield encounters both temporally and spatially varying conditions. At a given point on the surface of the spacecraft, the temporal variation of free stream conditions causes surface conditions such as heat flux and pressure to vary; heat flux and pressure both increase, peak, and then recede as the vehicle decelerates and descends through the atmosphere. A material's response to time-varying conditions at a particular surface location may be different than the response to the constant condition of an arc jet test, however. As a result of time-varying conditions, certain thermochemical phenomenon may only manifest in flight but not in ground testing at constant flow conditions. While physics-based modeling of material response attempts to account for the most relevant processes and influential applied environment parameters that affect material performance, gaps in modeling fidelity may only be revealed when comparing simulation results to data obtained under conditions that most closely approximate the anticipated flight environment.

---

<sup>1</sup> Senior Research Scientist, Aerothermodynamics Branch, MS 230-2, Associate Fellow AIAA.

<sup>2</sup> Chief Technologist, Entry Systems and Technology Division, MS 229-3, Associate Fellow AIAA.

<sup>3</sup> Senior Research Engineer, Thermophysics Facilities Branch, MS 229-4.

<sup>4</sup> Senior Engineer, Thermophysics Facilities Branch, MS 229-4, Senior Member AIAA.

<sup>5</sup> Engineering Supervisor, Thermophysics Facilities Branch, MS 229-4, Member AIAA.

<sup>6</sup> Senior Research Scientist, Entry Systems and Technology Division, MS 229-3, Associate Fellow AIAA.

<sup>7</sup> Research Scientist, Aerothermodynamics Branch, MS 230-2.

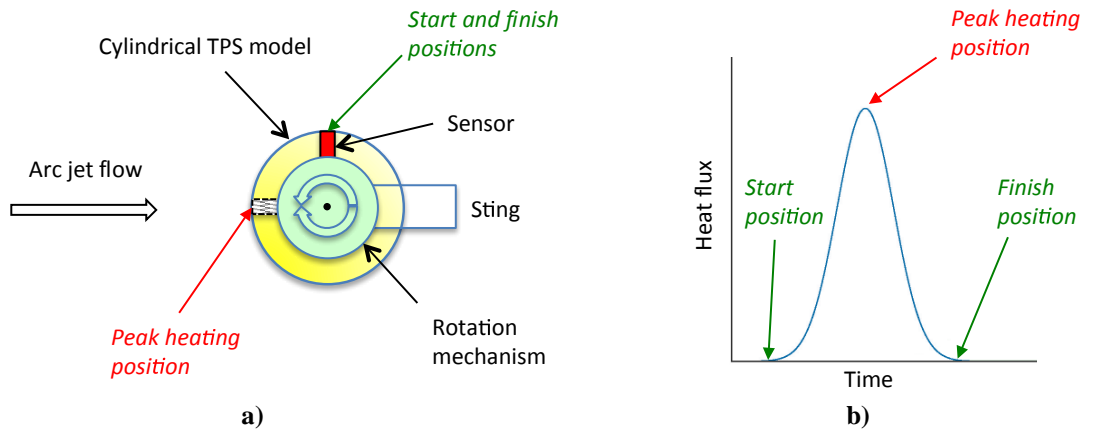


**Figure 1: a) Rotating arc jet test model concept. b) Time-dependent heat flux profile at sensor location on rotating test model.**

The goal for aerothermal analysts is to develop and validate modeling tools that can predict how a material perform will in flight – not just how the material will perform in the next arc jet test. Simulation development based on constant-condition arc jet testing methodologies is the foundational practice followed for physics-based modeling. But simulations developed from constant-condition arc jet testing may not capture critical thermophysical and thermochemical phenomena that, if known and modeled accurately, could ultimately influence design decisions. Achieving time-varying conditions in an arc jet flow can be accomplished by concurrently varying flow rate(s) and arc current. However, the ability to follow a profile can be a formidable challenge in an arc jet. Response times to flow rate and current changes may inhibit time-accurate replication of smoothly varying conditions which track the intended profile – the profile would be approximated by a small number of discrete step changes in conditions. Furthermore, for a particular facility configuration, the available range of flow conditions available during a single run may be insufficient to capture the full time-integrated material response behavior under investigation. An alternative approach is to operate the facility at a constant condition but take advantage of the varying heat flux and pressure distributions over the surface of a curved test model.

## II. Rotating test model concept

The concept utilizes a cylindrical arc jet test model that rotates on its axis, perpendicular to the flow direction, during a test run (Fig. 1a)). The heat flux and pressure at a single point on the model will increase to their peak values then decrease as a function of time as the point rotates towards and away from the stagnation point. The model size and constant arc jet operating condition are chosen such that the stagnation point heat flux matches the anticipated peak heat flux at a targeted location on an entry vehicle’s heat shield. Since the convective heat flux in flight spans from zero to its maximum and back to nearly zero (Fig. 1b)), the angular direction and instantaneous rate at which the model is rotated could be programmed to realize a time-varying heat flux profile that maps, as closely as possible, to the profile of the targeted location on the vehicle.

The MSL Entry, Descent, and Landing Instrumentation (MEDLI) project<sup>1</sup> for NASA’s Mars Science Laboratory (MSL) mission inspired development of this concept. The forebody heat shield of the MSL entry vehicle was embedded with MISPs (MEDLI Integrated Sensor Plugs) at several locations to measure in-depth temperatures and recession of the PICA (Phenolic Impregnated Carbon Ablator) heat shield material during hypersonic entry. The MISP technology was a natural fit for demonstration of the rotating test model approach as authentic time-varying conditions can be applied to the sensor plug to approximate the heat pulse encountered in flight.

With constant-condition arc jet testing, cold wall heat flux and pressure measurements from stream probes typically are used to anchor engineering or high-fidelity simulations of the arc jet stream and flow over the test model geometry. The test model simulations establish aerothermal environment boundary conditions for TPS material response calculations performed with analysis tools such as FIAT<sup>2,3</sup> or TITAN.<sup>4</sup> A similar approach could be used for a rotating test article – in this case the boundary conditions become time dependent in the reference frame of the rotating model.

### III. Rotating test model design

Moving the concept from an idea to a practical device started with the design of a motor-driven mechanism that operates while exposed to an arc jet stream. The outline of the mechanism design followed from the requirements of the test article. Those, in turn, were driven by the test objectives and test conditions. The requirements also addressed implementation of the concept – installation and operation of the mechanism, accommodation of test article instrumentation, and measurement of heat flux and surface pressure applied to the test article. The latter are critical for verifying test condition requirements and validating simulations used for post-test analyses.

#### A. Design considerations and requirements

An arc jet test is designed to achieve a prescribed set of environment conditions at a particular point on a test article. In addition to the test gas flow rate and arc current, the test article's size and shape, the arc jet's nozzle size, and the distance of the model from nozzle exit are the primary parameters to be specified in a test configuration.<sup>5</sup> The size of the test article relative to the core flow, and the ability of the facility's diffuser to capture the gas stream diverted by a test model (article and holder), also influence and constrain the choice of parameters in a test configuration. In the case of our rotating test article concept, the design of the mechanism that performs the rotation function was an important consideration in maintaining flexibility to meet test condition requirements.

To demonstrate the concept, we chose a moderate cold-wall heat flux of 140 W/cm<sup>2</sup> as the maximum value applied at the sensor location. That value also guided choices of test configuration parameters, primarily the TPS test article's diameter, arc jet nozzle size, and distance of the test article from the nozzle exit. Preliminary two-dimensional computational fluid dynamics (CFD) analyses of uniform flow over an infinite cylinder indicated that a 11.4 cm (4.5") diameter cylinder article paired with the 33 cm (13") exit diameter nozzle of the NASA Ames 60 MW Interaction Heating Facility (IHF) arc jet would adequately meet the heat flux requirement. The test article diameter was also sufficiently large to accommodate a standard MISP sensor plug<sup>1</sup> with only minor modifications.

To diminish confounding three-dimensional flowfield effects over the cylindrical test article, the shape of the mechanism's housing was designed as an extension of the model geometry. The combined length of the test article and mechanism housing was minimized to reduce flow blockage and ensure capture of the arc jet stream diverted by the assembly. A flow blockage test with a red oak wood model simulating the overall shape of the mechanism and test article verified that the IHF could accommodate this test configuration. With the overall concept established, the team designed the mechanism, test model, and characterization instrumentation.

##### 1. Test Environment Requirements

In addition to accommodating the physical size constraints described above, the mechanism was designed to operate under the vacuum conditions of the arc jet test chamber. While outgassing contamination from a motor was not of importance as it had no influence on the test environment, the ability of a motor to maintain function at rarefied pressures and moderate (~100 °C) temperatures for extended periods of time was essential. Since the mechanism would be impinged by the arc jet flow, water cooling of the mechanism's housing was also essential. The power supply and ionized gas flow of large-scale arc jet test facilities generate electromagnetic noise that can interfere with signal transmission, so electronic components and wiring used to control and monitor motion of the rotating test article was designed to operate under high levels of interference.

##### 2. Interface Requirements

Test article holders are typically custom-designed assemblies that attach to the model support system's sting arms using an adapter of a standard design. The sting arm provided a de-ionized cooling water manifold for the mechanism and a means to route instrumentation and motor control signals to the facility's data acquisition system. The design conformed to existing facility sting arm interface requirements while positioning the target location of the cylindrical test model on the nozzle centerline. The design also afforded access to the sting arm attachment, water cooling, and instrumentation interfaces during installation and setup.

##### 3. Operational Requirements

The key operational requirement for the mechanism design was a capability to rotate the test article according to a prescribed, pre-programmed angle vs. time schedule initiated on command by a test engineer. The rotation was bi-directional with a range  $\geq 90^\circ$ . The accuracy and precision of available stepper motor technology and gearing were sufficient to exceed a reasonable requirement of milliradian accuracy for article position. As correlation of test article material response with the time-varying applied environment was the motivation for the concept, the test article rotation angle was recorded concurrently with test article instrumentation signals.

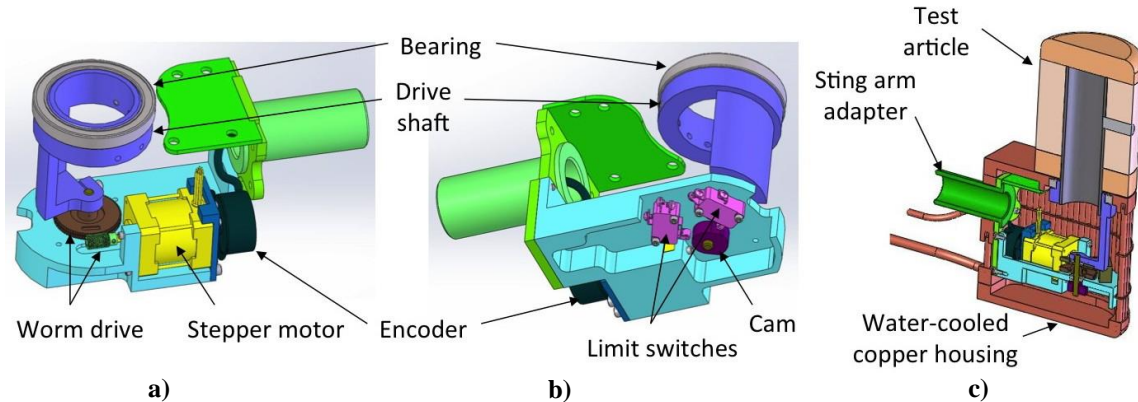


**Figure 2: Rotating mechanism. a) Top view. b) Bottom view. c) Section view of mechanism, housing, and test article.**

**B. Mechanism and control**

The rotating mechanism was based on a stepper motor and a worm drive (Fig. 2a)). The vacuum-rated stepper motor had a double-ended armature shaft, with one end connected to a worm and the other to an encoder. The drive shaft assembly for the test article was mounted perpendicular to the motor. This assembly consisted of an 80:1 anti-backlash worm gear mated to the worm, a notched drive shaft, and a cam that triggered forward and backward end-of-motion limit switches (Fig. 2b)). The notched drive shaft has a 50.8 mm (2.0”) diameter bore with radial set screws for attachment of a test model. The open volume between the drive shaft and the sting arm attachment was reserved for instrumentation wiring connections.

The water-cooled copper protected the mechanism during exposure. It was designed for convenient installation of instrumented test articles. The housing consisted of three separate water-cooled assemblies – main housing, a back, and an access panel. The torch-brazed assemblies were constructed from 6.35 mm (0.25”) diameter copper tubing and machined copper end manifolds. Each assembly had its own water supply and return connections to the model support arm’s cooling water system. The rotating mechanism was attached to the upper manifold of the

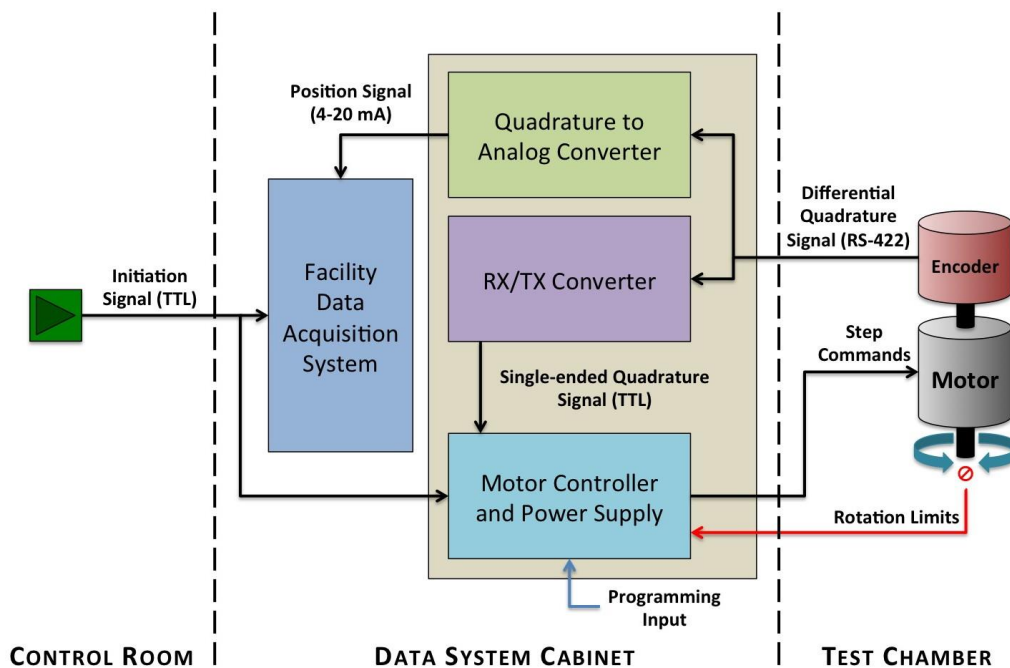


**Figure 3: Stepper motor control system block diagram.**

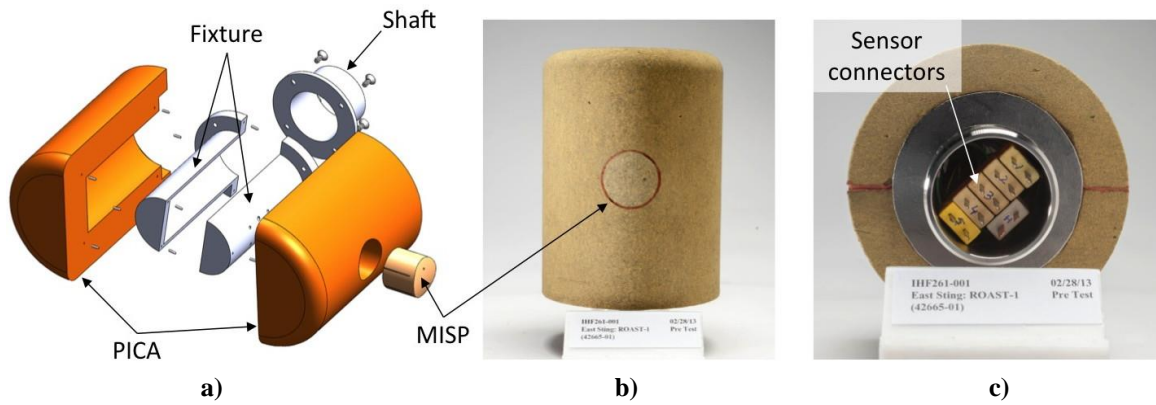


**Figure 4: Cylindrical TPS test article. a) Assembly view. b) Pre-test article with MISIP. c) End view of test article showing instrumentation connectors.**

main housing, which also incorporated the large ball bearing for the notched drive shaft.

A schematic of the motion control system design meeting the operational requirements described above is shown in Fig 3. The stepper motor was driven by a programmable controller and power supply. The encoder's differential quadrature position signal was converted to a single-ended signal compatible with the motor controller's input. The signal from a single-ended quadrature encoder could not be used because it was found to have insufficient strength for clear transmission through the cable between the controller and mechanism. It was also believed that the signal would have been too susceptible to electromagnetic interference from the arc jet. The encoder's differential output was also converted to an analog signal proportional to the motor's rotation so that the facility's data acquisition system could record the test article's angular position during exposure. The motor controller and two converters were built into a 19" rack housing and mounted in the facility's data system cabinet. Shielded wiring harnesses for the rotating mechanism, which included actuation, feedback, and limit switch signals, connected the mechanism to the rack-mounted motor control housing through the facility's instrumentation wiring infrastructure. Two identical rotating mechanisms were built, each with its own controller and signal conversion electronics.

A series of motion commands were written on a computer then uploaded to the controller and stored in the controller's non-volatile memory. The rotation sequence of the stored program was executed upon receiving a remote initiation signal from the arc jet test engineer in the facility control room.

### C. TPS test model and calorimeter

The cylindrical TPS test article was constructed from two machined billets of PICA. Figure 4a) shows an exploded assembly drawing of the test article. The two machined pieces were mated in a clamshell arrangement around an aluminum fixture to form a 15.2 cm (6.0") long, 11.4 cm (4.5") diameter cylinder. An adapter connected the test article assembly to the 50.8 mm (2.0") bore of the rotating mechanism's notched drive shaft. One of the PICA halves was bored out to accept a MISIP sensor plug.

The standard 33 mm (1.3") diameter MISIP has four Type K (chromel-alumel) thermocouples and one HEAT

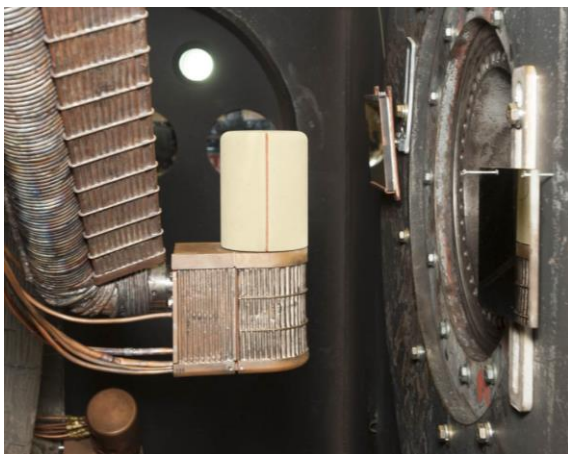


**Figure 5: Rotating mechanism and TPS test article installed in the IHF arc jet.**

(Hollow aErothermal Ablation and Temperature) sensor.<sup>1</sup> The thermocouples are at depths of 2.5 mm, 5.1 mm, 11.4 mm, and 17.8 mm (0.1", 0.2", 0.45", and 0.7", respectively) below the surface. Due to the curvature of the cylindrical PICA test article, the outer surface of the standard MISIP was machined to conform to the test article's curvature. The location of the thermocouples and HEAT sensor remained the same as those in the baseline design. A fifth Type K thermocouple was attached to the PICA/test fixture bondline, 31.8 mm (1.25") below the surface. Figures 4b) and 4c) are photos of a completed PICA test article and its end view showing the sensor connectors just inside the drive shaft adapter. The instrumentation wiring harness from the facility data system was routed through the sting arm and into the mechanism housing. The housing's removable access panel enabled instrumentation technicians to mate



**Figure 6: Instrumented copper cylinder for measurement of heat flux and surface pressure. Locations of the heat flux gauges and pressure ports are indicated.**

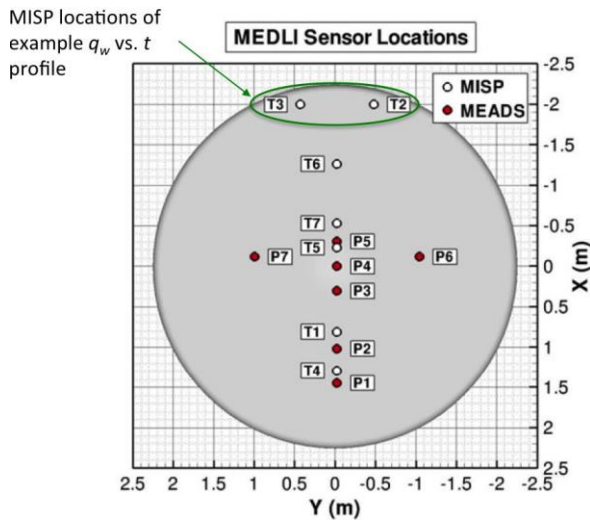


**Figure 7: MSL forebody heat shield map of MEDLI MISP and MEADS (Mars Entry Atmosphere Data System) sensors. The MISP T2/T3 locations were chosen for heat flux vs. time replication. From Reference 6.**

locations of the heat flux gauges and pressure ports. The heat flux gauges at 45° and 90° were offset by ±15 mm (0.6”) in the axial direction from the midplane to accommodate their depth and cooling water tubing within the interior cavity. The pressure ports at each of the three locations were also offset by 18 mm (0.73”) in the axial direction from the adjacent heat flux gauges.

#### IV. Rotating test model demonstration

The rotating test model concept was demonstrated in a series of tests in the NASA Ames IHF arc jet. A representative time-varying heat pulse was taken from MSL entry aerothermal calculations, based on MISP sensor T2 shown in Figure 7. In an attempt to replicate a plausible flight profile, the un-margined fully-turbulent calculations at MISP T2 were used. This sensor, located on the leeside shoulder, was expected to show the highest likely heating measurable by any of the seven MISPs.<sup>7</sup> MISP flight data confirmed that T2 (and T3) did experience the highest heating; however, reconstructed heat rates indicated that the actual peak heating at MISP T2 and T3 was likely lower than the profile selected for the demonstration test.<sup>8-10</sup> The predicted heat flux pulse at T2 peaked at 140 W/cm<sup>2</sup>, and is plotted in Figure 8a). In order to replicate, as closely as possible, this time-varying heat flux on the

the sensor connectors to the harness after the mechanism and model had been installed on the sting arm. Figure 5 shows one of the PICA test articles installed in the IHF prior to a test run. The rotating mechanism was attached to the model sting arm with the rotation axis oriented vertically.

Selection of arc jet facility operating parameters that will generate prescribed cold-wall heat fluxes and pressures to test articles is guided by experience and refined by iteration. Calibration measurements with stream probes of the same geometry as the test model are compared with requirements, and facility parameters are adjusted until measurements match requirements within achievable accuracy. In some cases a verified empirical relationship between different test model geometries can be applied to establish the necessary facility operating parameters. However, the more complex geometry of an offset rotating mechanism housing mated to a cylindrical test article had no traceable relationship to standard test model geometries. For this reason an instrumented copper test article of the same dimensions as the PICA test articles was designed and fabricated.

The instrumented copper cylinder characterized the heat flux and pressure distributions around the cylinder, not just at the stagnation point. Values of these distributions along an arc normal to the rotation axis became the time-varying conditions at a fixed point on the arc during test article rotation. Meaningful interpretation of time-varying material response data relied on validated simulations of heat flux and pressure distributions. Direct measurements of heat flux and pressure on the cylinder provided the necessary data for validation.

The uncooled copper cylinder was fitted with three water-cooled Schmidt-Boelter heat flux gauges and pressure ports. The gauge and port locations were clocked at 0°, 45°, and 90° relative to the stagnation point. The cylinder was mounted to the rotating mechanism but was designed not to rotate during its brief (3-4 s) exposure to the arc jet stream. Figure 6 shows the instrumented copper cylinder with arrows indicating the

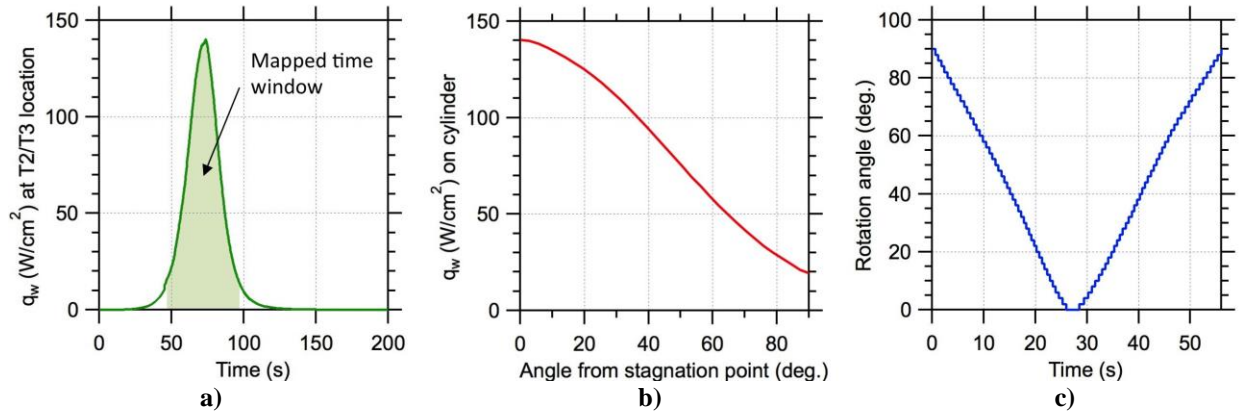


**Figure 8:** a) Predicted heat flux vs. time for MSL at the MEDLI T2/T3 location. b) Predicted heat flux distribution over cylinder as a function of angle for the 140 W/cm<sup>2</sup> test condition. c) Test article rotation angle vs. time obtained by mapping time-varying heat flux of a) to angular heat flux distribution of b). Only the shaded portion of a) was included in mapping the heat flux profile.

rotating TPS test article, a sequence of rotation angles as a function of time was prescribed for the rotation mechanism’s motion. That, in turn, required knowledge of the heat flux distribution along the path that the MISP sensor would travel during rotation. The engineering fidelity, two-dimensional CFD analysis of uniform flow over a 11.4 cm (4.5”) diameter infinite cylinder was sufficient for the purposes of this demonstration test. The arc jet free stream conditions simulated in the calculation were adjusted such that the cold-wall stagnation heat flux was approximately 140 W/cm<sup>2</sup>. The resulting heat flux distribution on the cylinder, indexed by angle, is plotted in Fig. 8b).

With the heat flux vs. time from the MSL entry simulation and the heat flux vs. angle from the arc jet test cylinder simulation, a correlation was computed to give the angular profile which would match the temporal heat flux at the MISP location on the cylinder to the temporal heat flux of the MSL heat pulse. Angular motion of the test article was limited from 0° to 90°. The time-varying heat pulse began with the MISP at 90° from the stagnation point. The cylinder rotated to 0° at the heat pulse peak, then returned to 90° at the end of the heat pulse. The results of the mapping are shown in Figure 8c). The heat flux is greater than zero at the 90° location, so the time window of Fig. 8a) mapped to the 90°–0°–90° sequence was shortened to begin and end at nonzero values of the predicted heat flux, as shown by the shaded region.

To simplify programming of the stepper motor controller for the purposes of this first demonstration, the angle vs. time correlation was discretized as a series of dwell times at 2° increments as seen in Fig. 8c). Prior to insertion of the mechanism in the stream, the controller started with the model positioned at 0° for alignment purposes. When commanded with a trigger signal, the controller moved the test article to the 90° position – ready for insertion of the mechanism into the stream – then waited for another trigger signal to start the programmed rotation sequence. Immediately upon confirmation that the sting arm had placed the mechanism at the test location, the test engineer initiated the test article rotation. The controller executed the sequence of 2° moves to 0° and back to 90°. The model support system was programmed to hold the mechanism in the stream for the duration of the rotation sequence. The facility data acquisition system recorded all the sensor signals prior to, during, and after the test article exposure. The data system also recorded the stepper motor rotation for time correlation of the test article’s angular position with sensor response.

**Table 1: Arc jet test conditions**

Facility Parameter	140 W/cm <sup>2</sup> condition	80 W/cm <sup>2</sup> condition
Main air (g/s)	110	100
Add air (g/s)	160	250
Arc current (A)	2200	2010
4.5” cyl stagnation heat flux (W/cm <sup>2</sup> )	149	73
Stagnation pressure (kPa)	7.8	8.6

In addition to the 140 W/cm<sup>2</sup> peak heat flux condition, a second condition with a peak of 80 W/cm<sup>2</sup> was also run. The second condition was chosen as a representative approximation of the maximum un-margined heat flux for MISP location T7. The second condition afforded an opportunity to assess differences in material response for two maximum heat fluxes following similar time-varying profiles.

The IHF is equipped with multiple model support sting arms. The two mechanisms were installed on two of the arms which enabled exposure of two test articles in each run. The test articles were located located 25.4 cm (10”) downstream of the nozzle exit plane with the cylinder midplane coincident with the nozzle axis. Six instrumented

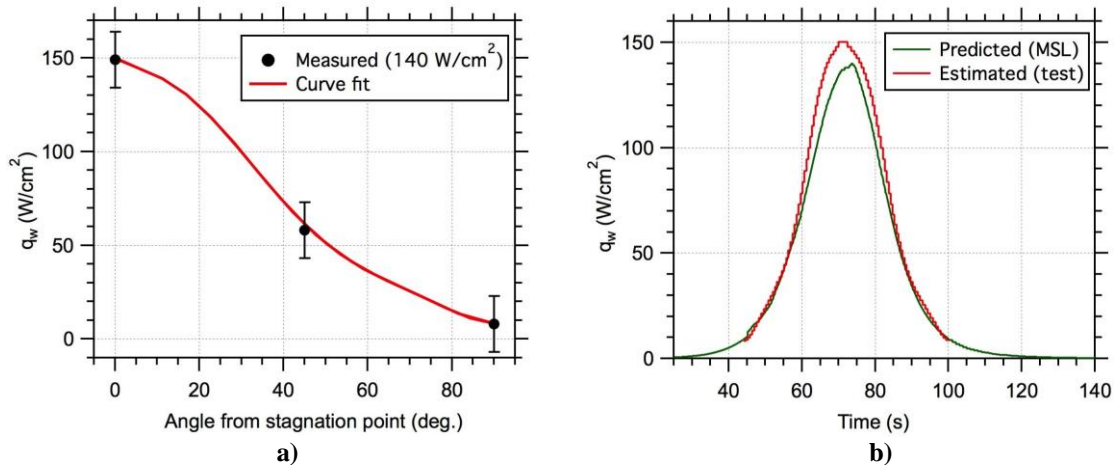


**Figure 9: a) Measured cold-wall heat fluxes on the instrumented copper cylinder for the 140 W/cm<sup>2</sup> condition. The curve fit was constrained by the as-measured 0° and 90° values to obtain an approximation of the angular heat flux distribution. b) Estimated time-varying cold-wall heat flux applied to MISP location of test article as determined from the heat flux distribution of a) and angle vs. time schedule of Fig. 8c). The target MEDLI T2/T3 heat flux (Fig. 8a)) is also shown for comparison.**

PICA test articles were built for this test. The demonstration test series was conducted in four runs with a total of eight model insertions – two for test condition calibration with the instrumented copper cylinder and six for the rotating PICA test articles (three at each condition). The stagnation (0° location) heat flux values confirmed that the requested test conditions were achieved with sufficient accuracy for this demonstration and that testing with the TPS models could proceed. The facility operating parameters and stagnation heat flux and pressure for the two test conditions are listed in Table 1.

The 0°, 45°, and 90° heat fluxes for the 140 W/cm<sup>2</sup> condition measured with the copper cylinder provided the means to establish better definition of the heat flux distribution on the cylindrical test articles. Figure 9a) shows the measured heat fluxes and a two-point constraint curve fit derived from the predicted engineering-fidelity angular distribution of Fig. 8b). The fitted function was then used with the rotation angles from the angle vs. time schedule executed during the tests (Fig. 8c)) to recover an approximation of the time-varying heat flux that was actually applied to the MISP location on the rotating test article (Fig. 9b)). In the future, the angular heat flux distribution, anchored to measured values, would be used to generate the rotation angle vs. time schedule to be executed by the rotating test articles.

A series of photos from one of the three PICA test article runs at the 140 W/cm<sup>2</sup> condition appears in Fig. 10. The succession of images shows the MISP plug rotating towards the stagnation point then back to the initial position as it experiences the transient heat pulse. The total exposure time was approximately 60 seconds. Figure 11 shows a thermal image of the test article just after peak heating, with the MISP rotating back toward the camera. The lee side of the cylinder could not be resolved from the background in the coldest region of the thermal image. The uniformity in temperature above and below the midplane qualitatively indicates that the cylindrical geometry of this test configuration minimizes three-dimensional effects near and within the region of interest.

In a conventional, constant-condition arc jet test, the surface temperature of a TPS material test article would rise monotonically until the temperature reached an equilibrium value or the article was removed. Once removed from the stream, the surface temperature would fall rapidly as the material cools. For the rotating arc jet test article, the time-varying heat flux applied to the MISP generated a different surface temperature response. The time histories of temperatures from the test article's thermocouples are plotted in Fig. 12. The duration of the test article exposure and programmed rotation is denoted in the plot. For both test conditions, the temperature measured by the first thermocouple nearest the surface peaked then began to fall during model exposure, which correlated with the applied heat flux pulse at the MISP location. This observation confirmed that the rotating test article concept functioned as intended – a time-varying heat flux applied to a TPS material created a response similar to what would be expected in flight.

A complete thermal analysis of the PICA/MISP test article material response is in progress. The time-dependent modeling approach differs from that of a conventional, constant-condition arc jet test because the test article moves in a rotating reference frame, requiring development of new modeling practices that account for spatiotemporal

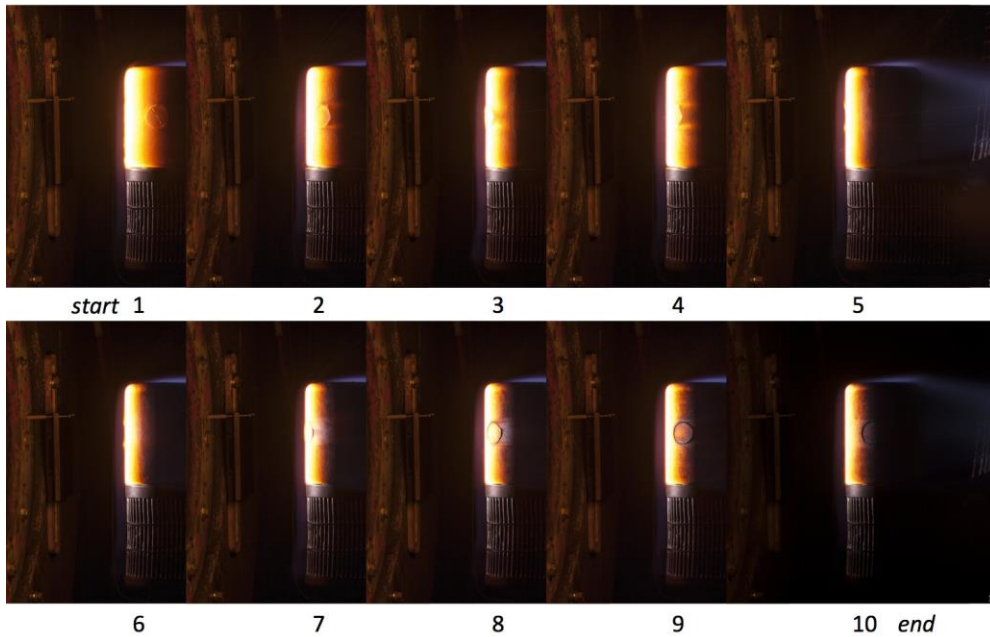


**Figure 10: Sequence of images from a test with an instrumented TPS test article. The flow is from left to right. The first image shows the test article just after insertion. The last images shows the test article at the end of the rotation sequence and just prior to retraction from the flow. The duration of the sequence was approximately 55 seconds.**

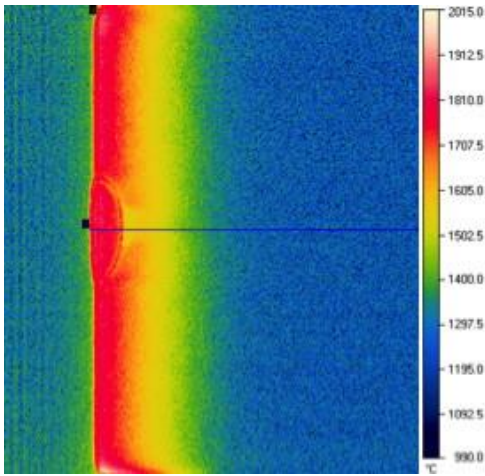


**Figure 11: Thermal image of a TPS test article at the 140 W/cm<sup>2</sup> condition. The image was acquired just after peak heating.**

variations in the applied aerothermal environment. We are also pursuing the inverse parameter estimation approach<sup>7-10</sup> whereby the time-varying applied environment and material response are reconstructed from the measured surface and in-depth temperature data. Taken together, both direct and inverse analysis approaches have the potential to improve our understanding of material response under time-varying conditions that better approximate flight.

## V. Conclusion

A new concept for TPS materials testing in arc jet facilities was developed and demonstrated. The approach utilized the spatial variation in aerothermal conditions on a curved test article to apply a time-varying condition at a point by rotating the article during a test. The concept was motivated by an aspiration to create testing methodologies that better simulate the aerothermal environments of atmospheric entry. The test configuration can be tailored to replicate the rise, peak, and fall in applied heat flux at a critical point on an entry vehicle's

TPS. In some cases, the configuration could be optimized to approximate a time-varying surface pressure profile while simultaneously replicating the heat flux profile at the target location. Applications include evaluation of a TPS material's in-depth response, ground testing of flight instrumentation, and validation of post-flight analysis techniques for flight data – all under time-varying conditions that approximate flight.

The concept was realized through the use of a programmable stepper motor that rotated a cylindrical test article during a constant-condition arc jet test. Pre-test analysis of the heat flux distribution over a cylinder provided the range of heat flux values on a locus of points that the target location on the test article would follow during rotation. The time-varying heat flux profile to be replicated was mapped to the spatial heat flux distribution over the cylinder. The test article's rotation profile (angle vs. time) could then be derived and programmed into the stepper motor controller. The concept was demonstrated in a series of arc jet tests using instrumented PICA cylindrical test articles.

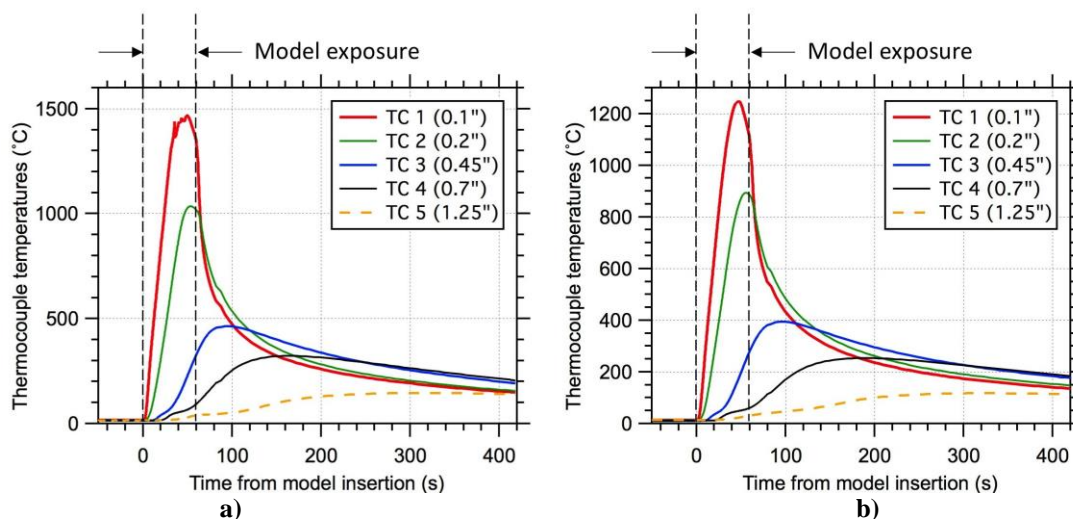


**Figure 12: Time histories of TPS test article sensors. TC 1 denotes the temperature from the MISP thermocouple at a depth of 2.5 mm (0.1"). a) 140 W/cm<sup>2</sup> condition. b) 80 W/cm<sup>2</sup> condition.**

Transforming the concept into a practical device drew upon the broad experience of the design team in supporting arc jet testing technology development efforts. This effort involved the mechanical design and fabrication of the mechanism, development of its operational and control procedures, and design and fabrication of instrumented test articles. The capabilities of the mechanism are general enough to be applied or extended to larger or differently shaped test articles.

### Acknowledgments

Support was provided by NASA's Hypersonics Project/Fundamental Aeronautics Program and MSL/MEDLI Project. E. Noyes, J. Mach, and D. Empey were funded under contract NNA09DB39C to Jacobs Technology. D. Prabhu and T. White were funded under contract NNA10DE12C to ERC, Inc. The authors thank M. Wright of NASA Ames, M. Munk of NASA Langley, and the engineers and technical staff of the Ames arc jet facility and TPS model development laboratory. The authors also thank A. Dyakonov, formerly of NASA Langley, for computational simulations during concept development.

### References

- <sup>1</sup>Bose, D., Santos, J.A., Rodriguez, E., White, T., Olson, M., and Mahzari, M., "Mars Science Laboratory Heat Shield Instrumentation and Arc Jet Characterization," AIAA Paper 2013-2778, June 2013.
- <sup>2</sup>Chen, Y.-K., and Milos, F.S., "Ablation and Thermal Analysis Program for Spacecraft Heatshield Analysis," *Journal of Spacecraft and Rockets*, Vol. 36, No. 3, 1999, pp. 475-483.
- <sup>3</sup>Chen, Y.-K., and Milos, F.S., "Two-Dimensional Implicit Thermal Response and Ablation Program for Charring Materials," *Journal of Spacecraft and Rockets*, Vol. 38, No. 4, 2001, pp. 473-481.
- <sup>4</sup>Chen, Y.-K., and Milos, F.S., "Three-Dimensional Ablation and Thermal Response Simulation System," AIAA Paper 2005-5064, June 2005.
- <sup>5</sup>Grinstead, J.H., Stewart, D.A., and Smith, C.A., "High enthalpy test methodologies for thermal protection systems development at NASA Ames Research Center," AIAA paper 2005-3326, May 2005.
- <sup>6</sup>Edquist, K.T., Dyakonov, A.A., Wright, M.J., and Tang, C.Y., "Aerothermodynamic Design of the Mars Science Laboratory Heatshield," AIAA Paper 2009-4075, June 2009.
- <sup>7</sup>Edquist, K., Hollis, B., Bose, D., White, T., and Mahzari, M., "Reconstruction of the Mars Science Laboratory Heatshield Aerothermodynamics," AIAA 2013-2781 44th AIAA Thermophysics Conference, San Diego, California, June 2013.
- <sup>8</sup>Bose, D., White, T., Santos, J., Feldman, J., Mahzari, M., and Edquist, K., "A Reconstruction of Aerothermal Environment and Thermal Protection System Response of the Mars Science Laboratory Entry Vehicle," AAS 13-311, AAS/AIAA Spaceflight Mechanics Meeting, Kauai, Hawaii, February 2013.
- <sup>9</sup>White, T., Mahzari, M., Bose, D., and Santos, J., "Post-flight Analysis of the Mars Science Laboratory Entry Aerothermal Environment and Thermal Protection System Response," AIAA 2013-2779, 44th AIAA Thermophysics Conference, San Diego, California, June 2013.
- <sup>10</sup>Mahzari, M., White, T., Braun, R., and Bose, D., "Inverse Estimation of Mars Science Laboratory's Entry Aerothermal Environment and Thermal Protection System Response," AIAA 2013-2780, 43rd AIAA Thermophysics Conference, San Diego, California, June 2013.